

# The influence of crystal–field effects on the electronic transport properties of heavy–fermion systems: a semiphenomenological approach

<sup>1</sup>M. Huth\* and <sup>2</sup>F. B. Anders

<sup>1</sup>*Institut für Physik, Johannes Gutenberg–Universität Mainz, 55099 Mainz, Germany*

<sup>2</sup>*Department of Physics, University of California, Davis, CA 95616-8677, USA*

*\*present address: Loomis Laboratory of Physics, University of Illinois, Urbana–Champaign, IL 61801-3080, USA*

(May 1, 1997)

## Abstract

The electronic transport properties of heavy–fermion systems were calculated based on a semiphenomenological approach to the lattice non–crossing approximation in the limit of infinite local correlations augmented by crystal–field effects. Within the scope of this calculation using the linearized Boltzmann theory in the relaxation time approximation the qualitative features of the temperature–dependent resistivity, the magnetoresistivity and the thermoelectric power can be successfully reproduced; this is exemplified by a comparison with experimental results on  $\text{CeCu}_2\text{Si}_2$ .

## I. INTRODUCTION

Strong electronic correlations are a crucial aspect of the physics of heavy-fermion systems. The local Coulomb repulsion of the 4f or 5f lattice sites causes the atomic part of the Hamiltonian to be of non-bilinear form. Consequently the hybridization of the local f-electrons with the itinerant states cannot be treated in a conventional Feynman perturbation theory [1]. Several different theoretical concepts have been developed during the last 10 to 15 years to treat this problem. These are rooted in the somewhat simpler Kondo problem or single-impurity problem that is now well-understood (for recent reviews see [2]). If the f-moments are localized on a regular lattice the problem is rendered even more difficult, since the mechanism of coherent scattering for temperatures much below the Kondo energy scale  $T_K$  has to be introduced in the theory adequately in order to describe the observed coherence effects in the electronic transport properties. The first fully self-consistent microscopic theory developed in this context is based on the lattice version of the Non-Crossing Approximation (NCA) [3] and is therefore called Lattice-NCA (LNCA) [4]. The LNCA is able to reproduce the basic aspects of coherent scattering at low temperatures, such as a quadratic dependence of the resistivity on temperature. Recently the NCA was extended by a systematic continuation of the perturbation expansion giving rise to an improved starting point for the lattice approximation in the LNCA scheme [5].

Considering the complicated nature of the LNCA and its numerical elaboration a simplified approach including the essential aspects of the Kondo lattice seemed to be helpful. For that reason a semiphenomenological description of crystal field effects in Kondo lattices based on the LNCA was developed which is also applicable to the dynamical mean field theory (for reviews see [6]). This approach is able to give further insight in the respective influences of the different relevant energy scales in heavy-fermion systems on the measured electronic transport quantities.

To begin with, the LNCA is briefly reviewed starting with the formulation of the Anderson-lattice Hamiltonian in a generalized form based on the irreducible representa-

tions of the point group of the crystal. The results are exemplified for a Kramers ion in a tetragonal crystal field. The derivation of the conduction electron Green function is based on a semiphenomenological approximation to the local excitation spectrum. Using the relation between the conduction electron Green function and the transport relaxation time the electronic transport properties are calculated within the linearized Boltzmann theory. Finally, the calculations are complemented by a comparison with experimental results.

## II. DESCRIPTION OF THE MODEL

The concept of the approximate treatment of the Anderson lattice for the transport properties was introduced by Cox and Grewe [7] and extended to magnetotransport by Lorek, Anders and Grewe [8]. It is based on the local approximation and uses the local T-matrix calculated with the NCA/LNCA describing a single scattering event of a conduction electron off the  $f$ -electrons. In the next section this approximate treatment will be briefly reviewed and completed by a consideration of the crystal field level scheme. The transport coefficients are calculated using the transport integral method of the linearized Boltzmann theory.

### A. The LNCA including the crystal field

The starting point of our derivation is given by the Anderson–lattice Hamiltonian. A spin–degenerate conduction electron band couples to localized crystal field split ionic states by means of hybridization matrix elements. Fluctuations on the ionic sites are limited to those between singly occupied or empty states, i. e. the repulsive interaction on the ionic sites is assumed to be infinite. The Hamiltonian is given by the following expression

$$\mathcal{H} = \sum_{\underline{k}\sigma} \epsilon_{\underline{k}\sigma} c_{\underline{k}\sigma}^+ c_{\underline{k}\sigma} + \sum_{\nu, \Gamma\alpha} E_{\Gamma\alpha} X_{\Gamma\alpha, \Gamma\alpha}^\nu + \sum_{\nu, \underline{k}\sigma, \Gamma\alpha} \left[ V_{0, \Gamma\alpha}(\underline{k}\sigma) e^{i\mathbf{k}\cdot\mathbf{R}_\nu} c_{\underline{k}\sigma}^+ X_{0, \Gamma\alpha}^\nu + \text{h. c.} \right]. \quad (1)$$

The first part describes the kinetic energy of the uncorrelated band electrons. The energy of occupied local states is given by the second part. Finally, the hybridization between local and itinerant states is formulated by the third part of the Hamiltonian.  $\Gamma$  denotes an irreducible representation of the point group of the crystal,  $\alpha$  a state of that representation and  $X_{\Gamma'\alpha',\Gamma\alpha}^\nu = |\Gamma'\alpha'^\nu \rangle \langle \Gamma\alpha^\nu|$  the Hubbard projection operator at the site  $\nu$ .

In the periodic Anderson model the T-matrix  $T_{\underline{k}\sigma}(z)$  is related to the local Green function  $F_{\Gamma\alpha,\Gamma\alpha}(\underline{k}, z)$  in the following way [9]

$$T_{\underline{k}\sigma}(z) = \sum_{\Gamma'\alpha',\Gamma\alpha} V_{0,\Gamma\alpha}(\underline{k}\sigma) F_{\Gamma'\alpha',\Gamma\alpha}(\underline{k}, z) V_{\Gamma'\alpha',0}^*(\underline{k}\sigma) \quad (2)$$

which can be written in a more compact form by using a matrix formalism

$$T_{\underline{k}\sigma}(z) = \underline{V}^t(\underline{k}\sigma) \underline{F}(\underline{k}, z) \underline{V}(\underline{k}\sigma) \quad (3)$$

introducing the hybridization vector  $\underline{V}^t(\underline{k}\sigma)$  and the Green function matrix  $\underline{F}(\underline{k}, z)$

$$\underline{V}^t(\underline{k}\sigma) \equiv (V_{\Gamma_1\alpha_1,0}^*(\underline{k}\sigma), V_{\Gamma_1\alpha_2,0}^*(\underline{k}\sigma), \dots, V_{\Gamma_n\alpha_n,0}^*(\underline{k}\sigma)) \quad (4)$$

$$\underline{F}(\underline{k}, z) \Big|_{\Gamma'\alpha',\Gamma\alpha} \equiv F_{\Gamma'\alpha',\Gamma\alpha}(\underline{k}, z) \equiv \frac{1}{N} \sum_{\nu} e^{i\mathbf{k}\cdot\mathbf{R}_{\nu}} \ll X_{0,\Gamma'\alpha'}^{\nu}(\tau) X_{\Gamma\alpha,0}^0 \gg. \quad (5)$$

( $N$ : number of lattice sites)

With the exact equation of motion [12] for the conduction electron Green function

$$G_{\underline{k}\sigma}(z) = G_{\underline{k}\sigma}^{(0)} + G_{\underline{k}\sigma}^{(0)}(z) T_{\underline{k}\sigma}(z) G_{\underline{k}\sigma}^{(0)}(z) \equiv \frac{1}{z - \epsilon_{\underline{k}\sigma} - \Sigma_{\underline{k}\sigma}(z)} \quad (6)$$

we obtain the following expression for the band self-energy [9]:

$$\begin{aligned} \Sigma_{\underline{k}\sigma}(z) &= \frac{\underline{V}^t(\underline{k}\sigma) \underline{F}(\underline{k}, z) \underline{V}(\underline{k}\sigma)}{1 + G_{\underline{k}\sigma}^{(0)} \underline{V}^t(\underline{k}\sigma) \underline{F}(\underline{k}, z) \underline{V}(\underline{k}\sigma)} \\ &= \underline{V}^t(\underline{k}\sigma) \underline{F}(\underline{k}, z) \underline{V}(\underline{k}\sigma) \sum_{\ell=0}^{\infty} (-1)^{\ell} \left[ G_{\underline{k}\sigma}^{(0)} \underline{V}^t(\underline{k}\sigma) \underline{F}(\underline{k}, z) \underline{V}(\underline{k}\sigma) \right]^{\ell} \\ &= \underline{V}^t(\underline{k}\sigma) \underline{F}(\underline{k}, z) \sum_{\ell=0}^{\infty} (-1)^{\ell} \left[ \underbrace{V(\underline{k}\sigma) G_{\underline{k}\sigma}^{(0)} V^t(\underline{k}\sigma)}_{\equiv \underline{\Lambda}(\underline{k}\sigma, z)} \underline{F}(\underline{k}, z) \underline{V}(\underline{k}\sigma) \right]^{\ell} \\ &= \underline{V}^t(\underline{k}\sigma) \underline{F}(\underline{k}, z) \frac{1}{\underline{\mathbb{1}} + \underline{\Lambda}(\underline{k}\sigma, z) \underline{F}(\underline{k}, z)} \underline{V}(\underline{k}\sigma) \end{aligned} \quad (7)$$

The aim of the LNCA is to obtain an approximate expression for the T-matrix and local Green function [4]. Unlike the NCA, in the lattice the formal delocalization of a local f-electron via hybridization into a band electron state may be followed by additional scattering events on different lattice sites before the re-localization into any local state takes place. In order to allow for these scattering processes the concept of the effective lattice site is introduced (all quantities referring to it are indicated with a tilde). The scattering is subdivided into local and nonlocal events, with the hybridization events starting and ending at a local lattice site, respectively. The summation of all pseudo-local scattering events results in the scattering matrix  $\underline{V}^t(\underline{k}\sigma)\underline{\tilde{F}}(z)\underline{V}(\underline{k}\sigma)$  of an effective site. Accounting for the exclusive-site condition only for subsequent hybridization events the effective site Green function  $\underline{\tilde{F}}$  determines the local Green function according to [4]

$$\underline{F}(\underline{k}, z) = \frac{1}{\underline{\tilde{F}}(z)^{-1} - (\sum_{\sigma} \underline{\Lambda}(\underline{k}\sigma, z) - \underline{\Lambda}(z))} \quad (8)$$

with the definition

$$\underline{\Lambda}(z) \equiv \frac{1}{\#k} \sum_{\underline{k}\sigma} \underline{\Lambda}(\underline{k}\sigma, z) \quad (9)$$

Inserting equation (8) in equation (7) yields the following expression for the band self-energy that is central for the discussion of the transport properties within the scope of the linearized Boltzmann transport theory:

$$\Sigma_{\underline{k}\sigma}(z) = \underline{V}^t(\underline{k}\sigma) \frac{1}{\underline{\tilde{F}}(z)^{-1} + \underline{\Lambda}(z) - \underline{\Lambda}(\underline{k} - \sigma, z)} \underline{V}(\underline{k}\sigma) \quad (10)$$

Note the fact that even a local approximation like the LNCA can include the leading anisotropies in the conduction electron self-energy by using an angular dependent hybridization vector  $\underline{V}(\underline{k}\sigma)$ .

### B. Example: Three doublets; Kramers ion in tetragonal crystal field

For further discussion we consider the level scheme of a Kramers ion (e. g.  $\text{Ce}^{3+}$ ) in a tetragonal crystal field. In this case the Hund ground state multiplet  $J = 5/2$  splits

into three magnetic doublets. The hybridization is assumed to be spin-conserving without  $\underline{k}$ -dependence. Since the local pseudo-spin is a good quantum number, the hybridization couples only to one crystal field eigenstate in either of the three doublets for a given band electron spin direction. Consequently, the hybridization matrix is block diagonal and the  $6 \times 6$ -matrix decomposes into two  $3 \times 3$ -matrices with vanishing matrix elements in the upper/lower block matrix for local down/up spin direction. Since the band electron Green function has to be diagonal in the spin the same structure is given for the matrix  $\underline{\underline{\Lambda}}(\underline{k}\sigma, z)$  resulting again in a block diagonal form of  $\underline{\underline{\Lambda}}(z)$ . Finally, the effective site Green function matrix is diagonal due to the local hybridization. As a consequence the band self-energy decomposes for a given band electron spin into a sum of the self-energy contributions for the three doublet states

$$\Sigma_{\underline{k}\sigma}(z) = \sum_{j=1}^3 \frac{V_j^2 \tilde{F}_j(z)}{1 + \tilde{F}_j(z) \Lambda_{jj}(z)}. \quad (11)$$

A crossover to the single impurity Kondo effect can be accomplished by furnishing the scattering matrix with a prefactor  $c_{imp}$  that represents the concentration of the magnetic impurities

$$V_j^2 \tilde{F}_j(z) \rightarrow c_{imp} V_j^2 \tilde{F}_j(z) \quad (12)$$

After the expansion of the band self energy in equation (11) with respect to the small quantity  $c_{imp}$  the following result is obtained

$$\Sigma_{\underline{k}\sigma}(z) = c_{imp} \left( \sum_{j=1}^3 V_j^2 \tilde{F}_j(z) \right) \quad (13)$$

### C. Approximate treatment of the LNCA

The local excitation spectrum is given by the spectral functions  $1/\pi \cdot \text{Im}\tilde{F}_j(z)$ . The dominant influence on the transport properties is exerted by the many particle resonance structure near the Fermi surface. In the following this resonance is approximated by a Lorentzian curve

$$\tilde{F}_j(\omega) = \frac{a(T/T_{Kj})}{\omega - \eta_j - i\gamma_j} \quad (14)$$

which is in good correspondence to the results of a self-consistent solution within the PNCA procedure [5]. The low energy scale  $T_{K0}$  determines both the width  $\gamma = \pi/(2N + 1) \cdot k_B T_{K0}$  and the position  $\eta = k_B T_{K0}$  of the main resonance. The exact position of the resonance is difficult to specify accurately since new results within the PNCA reveal a shift of the resonance structure towards the Fermi energy in accordance with Friedel's sum rule for a decreasing degeneracy  $N_j$ , unlike the former NCA result [5]. The position and width of the  $N_j$  degenerated excited crystal field levels are given by  $\Delta_{0j} + T_{K0}$  and  $\gamma_j = \pi/(2N_j + 1) \cdot k_B T_{Kj}$  ( $\Delta_{0j}$  crystal-field splitting), respectively.

As is well-known from renormalization theory the low temperature properties of a Kondo system are dominated by the low temperature energy scale  $T_K$ . The argument of the temperature-dependent function  $a(T/T_{Kj})$  is therefore given by a relative temperature for the respective crystal field levels. All calculations performed in the following sections are based on the following temperature dependence

$$a(T/T_{Kj}) = \begin{cases} \frac{\gamma_i}{\Delta_j} (1 - b(T/T_{Kj})^2) & : T \ll T_{Kj} \\ a_0 \left(1 - \frac{\ln(T/T_{Kj})}{\sqrt{(\ln(T/T_{Kj}))^2 + \pi^2 S_j(S_j+1)}}\right) & : T \geq T_{Kj} \end{cases} \quad (15)$$

The quadratic temperature dependence for  $T \ll T_{Kj}$  is motivated by the Fermi liquid character of the quasi-particle excitations at low temperature. The prefactor  $\gamma_i/\Delta_j$  ( $\Delta_j = \pi V_j^2 N(\epsilon_F)$  Anderson width) is a consequence of the limiting behavior of the local density of states for  $T \rightarrow 0$  [13]

$$N_j(\omega) = -\frac{1}{\pi} \text{Im} \tilde{F}_j(\omega - i\delta) = \frac{\gamma_j^2}{\pi \Delta_j [(\omega - \eta_j)^2 + \gamma_j^2]} \quad (16)$$

It reflects the many body nature of the resonance: only a fraction of  $\sum_j \gamma_j/\Delta_j < 1$  of  $f$ -electrons participate in the scattering. In the temperature region  $T \geq T_{Kj}$  we use the results of the parquet diagram expansion of the Nagaoka-Suhl equations for the sd-model [14]. The parameters  $a_0$  and  $b$  are fixed by adjusting equation (15) to the temperature dependence of the resonance height within the PNCA procedure ( $N_j = 2$ ). In the region between the low

temperature and high temperature limiting cases a polynomial fit based again on the PNCA result [5] is used.

The influence of a magnetic field on the transport properties can be accounted for by introducing a Kondo field  $B_{Kj}$  that is given by the following relation for the respective crystal field level

$$k_B T_{Kj} = \mu_j B_{Kj} \quad (17)$$

The argument of the function  $a(x_j)$  is now given by a generalized form that includes temperature and field on an equal base and guarantees an isotropic field dependence in accordance with the assumed  $\underline{k}$ -independent hybridization

$$x_j = \sqrt{\left(\frac{T}{T_{Kj}}\right)^2 + \left(\frac{B}{B_{Kj}}\right)^2} \quad (18)$$

Within the Lorentz approximation of the effective site Green function a Zeeman splitting of the crystal field states has to be taken into account

$$\tilde{F}_j(\omega) = \frac{a(x_j)}{\omega - (\eta_j + \mu_j B) - i\gamma_j} \quad (19)$$

Nevertheless, in the paramagnetic phase of the model we expect that there is only one low temperature energy scale, the lattice Kondo temperature, which we set equal to  $T_{K0}$ . Equation (18) is only a natural way of parameterization of the decrease of the quasi-particle spectral weight with temperature or magnetic field and does not reflect a scaling law in the strict sense. Additional low energy scales like the Néel temperature [10] or the superconducting  $T_c$  [11] can be calculated within the LNCA by analyzing the residual quasi-particle interactions [4].

#### D. Relation to transport theory

Based on the results of the preceding sections the band electron Green-function is now used to give explicit expressions for different electronic transport properties. Within the



Green–function formalism of the transport theory a comparison with the relaxation time approximation of the linearized Boltzmann equation for the isotropic (cubic) case gives the following expression for the relaxation time [15]

$$\tau_\sigma(z) = \int_{\text{band}} [\text{Im}G_\sigma(\omega, z)]^2 d\omega \quad (20)$$

where the  $\underline{k}$ –dependence is averaged out.

This integral can be solved analytically for a symmetric energy band of the width  $2D$  yielding

$$\begin{aligned} \tau_\sigma(z = x - i\delta) &= \frac{\hbar}{\pi} \int_{-D}^D \left( \text{Im} \frac{1}{x - i\delta - \omega - \Sigma_\sigma(x - i\delta)} \right)^2 d\omega \\ &= \frac{\hbar}{2\pi} \left\{ \frac{\omega - (x - \text{Re}\Sigma_\sigma(x - i\delta))}{[x - \text{Re}\Sigma_\sigma(x - i\delta) - \omega]^2 + [\text{Im}\Sigma_\sigma(x - i\delta)]^2} \right. \\ &\quad \left. + \frac{1}{\text{Im}\Sigma_\sigma(x - i\delta)} \arctan \left[ \frac{\omega - (x - \text{Re}\Sigma_\sigma(x - i\delta))}{\text{Im}\Sigma_\sigma(x - i\delta)} \right] \right\} \Big|_{-D}^D \end{aligned} \quad (21)$$

In the Fermi–liquid regime for  $T \rightarrow 0$  the quasi-particle lifetime at the Fermi energy diverges resulting in  $\text{Im}\Sigma_\sigma(x - i\delta) \rightarrow 0$  and the second part in equation (21) dominates the relaxation time:

$$\tau_\sigma(z = x - i\delta) \simeq \frac{\hbar}{2\text{Im}\Sigma_\sigma(x - i\delta)} \quad (22)$$

Summing the spin–dependent relaxation times over the spin index leads to the total transport relaxation time

$$\tau(z = x - i\delta) = \sum_\sigma \tau_\sigma(z = x - i\delta). \quad (23)$$

This can be used to determine several transport quantities like the specific resistivity  $\rho$ , the thermopower  $S$  and the Hall coefficient  $R_H$  based on the transport integrals  $L_{mn}$  [16]:

$$L_{mn} = \int_{-\infty}^{\infty} \left( -\frac{\partial f}{\partial \omega} \right) \tau^m(\omega) (\hbar\omega)^n d\omega \quad (24)$$

$$\rho = \frac{6\pi^2 m^*}{e^2 k_F^3} \frac{1}{L_{10}} \quad (25)$$

$$S = -\frac{1}{|e|T} \frac{L_{11}}{L_{10}} \quad (26)$$

$$R_H = -\frac{2}{ne} \frac{L_{20}}{L_{10}^2} \quad (27)$$

To conclude this section we give an explicit expression for the matrix  $\Lambda_{jj}(z)$  that is needed to calculate the band self-energy in equation (11). For a Gaussian density of states symmetric around the Fermi energy  $\rho(\epsilon) = \rho(\epsilon_F) \exp(-\omega^2/D^2)$  the  $\underline{k}$ -sum in  $\Lambda_{jj}(z)$  can be performed as an energy integral

$$\Lambda_{jj}(z) = \frac{1}{\#\underline{k}} \sum_{\underline{k}\sigma} \frac{V_j^2}{z - \epsilon_{\underline{k}\sigma}} = -i\pi V_j^2 \rho(\epsilon_F) w(z/D) \quad (28)$$

with the error function  $w(z/D)$  [17]. Since the energy width of the Kondo resonance is given by the small energy scale  $k_B T_{Kj} \ll D$  the approximation  $w(x \ll 1) \simeq 1$  can safely be used; this leads to

$$\Lambda_{jj}(z) \simeq -i\pi V_j^2 \rho(\epsilon_F) = -i\Delta_j \quad (29)$$

Consequently, within the three doublet scenario, the calculation of the transport quantities in the subsequent section is based upon the following self-energy:

$$\Sigma_\sigma(z = \omega \pm i\delta) = \sum_{j=1}^3 \frac{V_j^2 \tilde{F}_j(\omega \pm i\delta)}{1 \mp i\tilde{F}_j(\omega \pm i\delta)\Delta_j} \quad (30)$$

In the low temperature region equation (30) reflects Matthiessen's law, according to which the resistivity is proportional to the sum of the inverse relaxation times.

### III. COMPARISON WITH EXPERIMENTAL RESULTS

In the following we compare the results of the model calculation with the transport properties of the heavy-fermion system  $\text{CeCu}_2\text{Si}_2$ . In  $\text{CeCu}_2\text{Si}_2$  the crystal-field splitting between the low lying Kramer's doublet and two energetically-degenerated excited doublets is much larger than the low temperature energy scale  $T_{K0}$  [18]. Possible magnetic exchange scattering contributions to the resistivity are neglected. Unlike the crystal-field splittings  $\Delta_{0j}$  and the Kondo temperature  $T_{K0}$ , the Kondo temperatures of the excited doublets  $T_{Kj}$  and the corresponding Anderson widths of the respective levels  $\Delta_j$  are not known. In order to derive Anderson widths which are consistent with the fixed Kondo temperature of the

ground doublet and the Kondo temperatures of the excited doublets the so called "poor man's" scaling result [2]

$$k_B T_K = \sqrt{D\Delta} \exp(-\pi|\epsilon_f|/2\Delta) \quad (31)$$

is used with fixed values for the cutoff parameter  $D = 2.5$  eV and the position of the localized f-level  $\epsilon_f = -2$  eV (typical values). For simplicity we assume equal Kondo-temperatures  $T_{K1} = T_{K2}$  for the energetically-degenerated excited two doublets. The Kondo temperature for the ground doublet  $|0 \rangle = -\eta | \pm 5/2 \rangle + \sqrt{1-\eta^2} | \mp 3/2 \rangle$  is set to 9 K according to reference [19] and  $\eta = 0.467$  [18]. The crystal-field splittings are known from inelastic neutron scattering to be  $\Delta_{01} = \Delta_{02} = 350$  K for both excited levels  $|1 \rangle = \sqrt{1-\eta^2} | \pm 5/2 \rangle + \eta | \mp 3/2 \rangle$  and  $|2 \rangle = | \pm 1/2 \rangle$ , respectively. In cubic symmetry  $\eta = \sqrt{1/6} = 0.408$  and  $|1 \rangle$  and  $|2 \rangle$  would form the  $\Gamma_8$  quartet. Finally, the density of states at the Fermi level  $N(\epsilon_F)$ , the absolute value of Fermi wave vector  $k_F$ , the effective mass of the non-correlated band electrons, and the number density of charge carriers  $n$  are chosen as 1/eV-states,  $0.5/\text{\AA}$ ,  $8m_e$  ( $m_e$ : free-electron mass), and  $2.5 \cdot 10^{22}/\text{cm}^3$ , respectively. The choice of these parameters is guided by typical values for d-metals so as to give a good correspondence with the measured resistivity. Additionally we neglected the temperature dependency of the Lorentzian widths  $\gamma_i$  in order to maintain the lowest possible set of parameters. The maxima due to higher crystal-field states will therefore appear more pronounced. The following paragraph will show that the simplifying assumption of an isotropic band structure results in quantitative differences between the calculated and experimentally-determined higher-order transport coefficients. Nevertheless, the aim of the present calculation is to give a qualitative correspondence.

In figure 1 a representative temperature-dependent resistivity curve is contrasted with the model calculation for different Kondo temperatures of the excited doublets. In order to facilitate a comparison with the experimental data a residual resistivity of  $20 \mu\Omega\text{cm}$  and the phononic resistivity contribution of a  $\text{LaCu}_2\text{Si}_2$  reference-sample [20] was added to the calculated curves.

## FIGURES

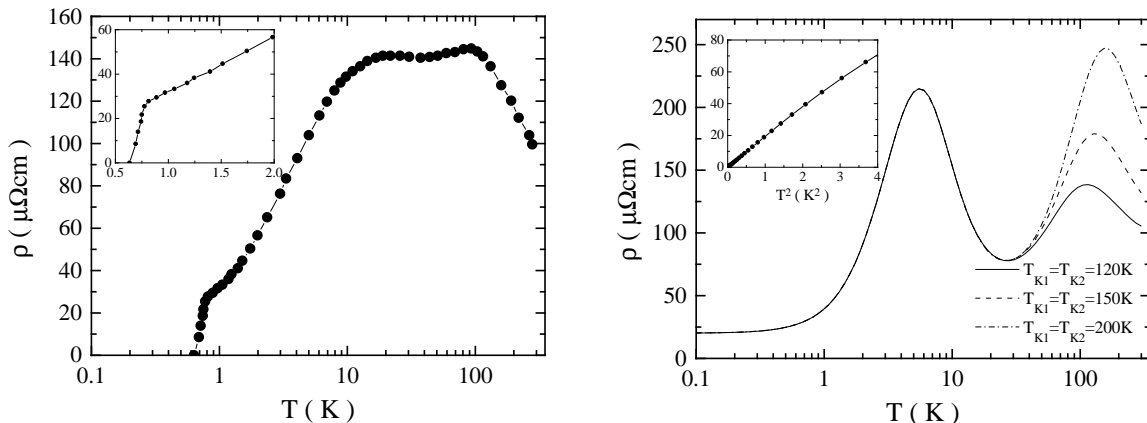


FIG. 1. Comparison of the temperature dependent resistivity of  $\text{CeCu}_2\text{Si}_2$  (left) with the model calculation (right). The inset on the right shows the calculated resistivity without residual resistivity and phonon contribution as a function of  $T^2$ . The resistivity data is taken from reference [20].

The qualitative correspondence is best for an excited doublet Kondo temperature of about 120 K as far as the position of the high temperature maximum in the resistivity is concerned. Interesting enough, the width of the observed crystal-field transition by Goremychkin et al. [18] is about 100 K due to the strong interactions of the f-electrons with the conduction band in good correspondance with our estimate of the Kondo temperature of the excited doublets.

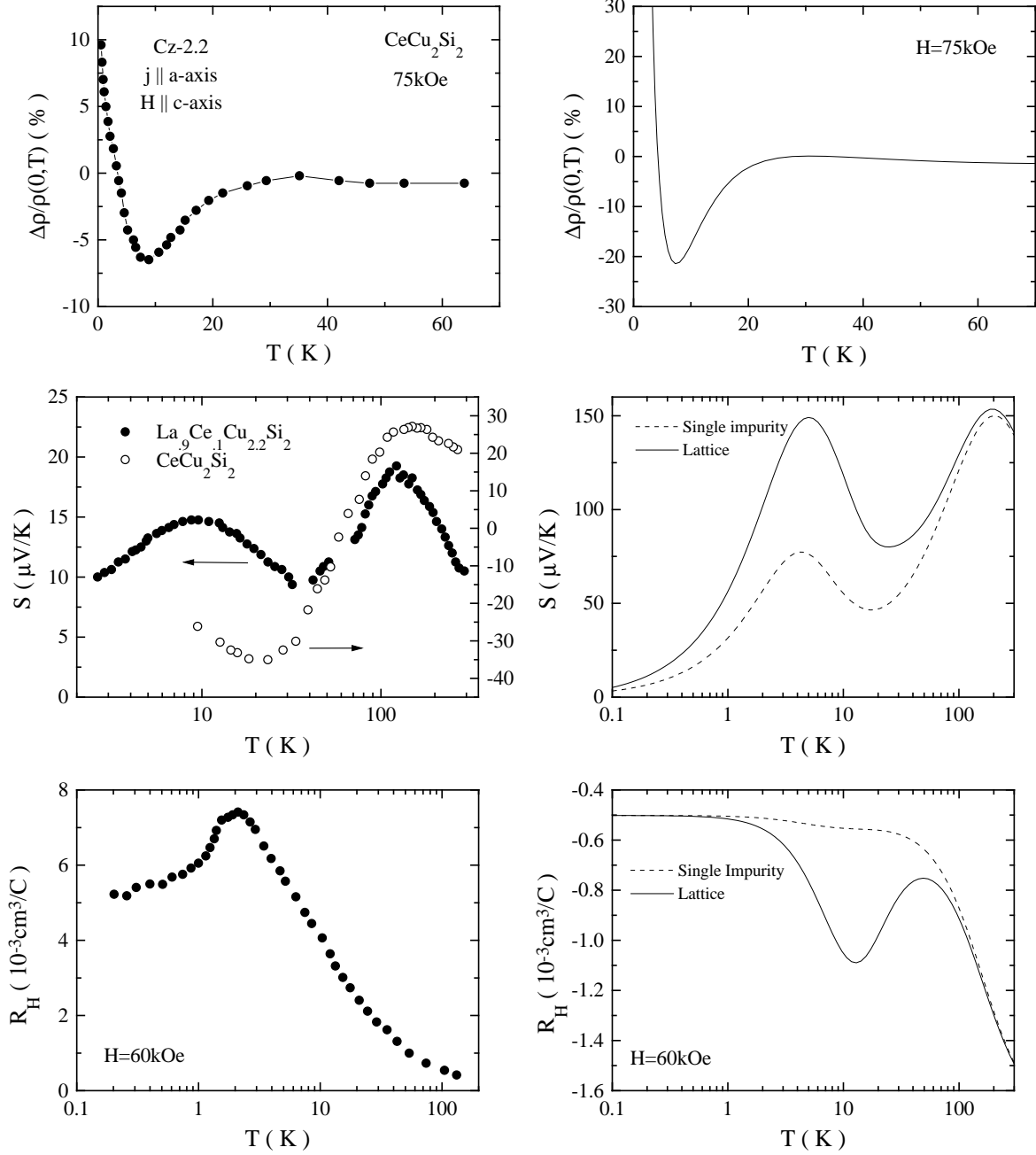


FIG. 2. Comparison of the temperature dependence of the magnetoresistivity [20], the thermoelectric power [21] ( $\text{CeCu}_2\text{Si}_2$ ) and [28] ( $\text{La}_{0.9}\text{Ce}_{0.1}\text{Cu}_{2.2}\text{Si}_2$ ), and the Hall coefficient [22] of  $\text{CeCu}_2\text{Si}_2$  (left) with the model calculations (right).

The low temperature maximum is more pronounced in the calculation. This is also true for  $\text{CeCu}_2\text{Si}_2$  samples with lower residual resistivity. The resistivity data of reference [20] was primarily taken since this represents a common feature of disordered Kondo lattices. With

increasing disorder in the system a distribution of hybridization strengths and positions of the local  $f$ -states is generated that cause a much broader distribution of Kondo temperatures according to the exponential dependence in equation (31). A distribution of Kondo temperatures might cause a significant rounding of the low temperature maximum. Due to electronic correlations the disorder-induced scattering rates grow faster than in uncorrelated systems. As a consequence, the coherent scattering part is reduced and the influence of disorder cannot be accounted for by a simple increase in the residual resistivity [25]. As shown in the inset of figure 1 (right) the low temperature part of the calculated resistivity follows a quadratic temperature dependence, as is expected in the Fermi-liquid regime. The low temperature resistivity of reference [20] reveals an interesting deviation from the quadratic behavior following a linear dependence. This might be caused by a quantum critical point in  $\text{CeCu}_2\text{Si}_2$  as recently discussed by Steglich et al. [28].

Based on the fixed parameter set with  $T_{K1} = T_{K2} = 120$  K figure 2 shows a comparison of several additional transport quantities as function of temperature. The left part represents experimental data from various references whereas the right part shows the calculated quantities.

The calculated magnetoresistivity is in good correspondence with the experimental data. Even the shallow maximum around 30 K caused by the excited crystal-field states is reproduced. Quantitatively the magnetoresistivity at low temperatures reaches 800% in the calculation (with  $20 \mu\Omega\text{cm}$  residual resistivity) whereas the experimental value is 10%. The reason for the reduced magnetoresistivity in the experimental data might also be traced back to the same influence of disorder on the coherent scattering part in the resistivity. Furthermore the calculation does not include possible band-structure effects.

According to the calculation the Seebeck coefficient shows no sign-reversal; this is in contradiction to the experimental result. Furthermore the low temperature maximum does not appear in the experimental data. Furthermore, the absolute values in the calculation are significantly higher. This could be attributed to a disorder-induced smoothening of the sharp features at the Fermi level in the samples. Some general remarks seem to be appropriate here.

The temperature dependence of the thermopower of heavy-fermion systems shows a wide variety of different features. In the trivalent cerium systems a sign reversal with a negative low temperature minimum is a common feature in concentrated systems. Recently Kim and Cox [27] discussed the possible realization of a two-channel Kondo impurity model in  $\text{Ce}^{3+}$  predicting a large negative thermopower in a cubic crystal symmetry and non-Fermi-liquid signatures in thermodynamic quantities. In dilute Cerium systems, however, a negative thermopower has never been observed. In recent measurements on  $\text{La}_{0.9}\text{Ce}_{0.1}\text{Cu}_{2.2}\text{Si}_2$  [28] a clearly positive thermopower is observed which is in strikingly good qualitative agreement with our calculation (see single-impurity calculation of  $S(T)$  in figure 2). For temperatures  $T \geq T_K$  the lattice and the impurity thermopower calculated within our model are very similar since coherence no longer plays a role and the impurity concentration explicitly cancels in equation 26. On the other hand the thermopower sensitively measures the asymmetry of the scattering rate above and below the chemical potential. In our opinion the negative thermopower of  $\text{CeCu}_2\text{Si}_2$ , which is still not properly understood, points towards additional lattice effects not included in our model. Besides a possible influence of the band structure non-local quasiparticle interactions, which are not contained in the local approximation, cause significant renormalizations of the one-particle properties; this is part of the LNCA concept [4]. These interactions mediate short-range antiferromagnetic fluctuations whose correlation length can grow with decreasing temperature. Assuming a quantum critical point ( $T_N \rightarrow 0$ ) the fluctuations can account for the observed non-Fermi-liquid behavior in  $\text{CeCu}_2\text{Si}_2$  above the superconducting  $T_c$  [28].

With increasing valence instability a crossover to an overall positive thermopower with a second low temperature maximum is observed (see e. g. in  $\text{CeRu}_2\text{Si}_2$  [26]). One possible reason for the negative component of the thermopower is given by intersite spin-interactions. Consequently, due to the onset of real charge fluctuations on the f-sites the negative part of the thermopower is suppressed [29]. Spin-spin interactions are not included in the calculation so the qualitative feature with two maxima in the calculated thermopower might be more representative of systems like  $\text{CeRu}_2\text{Si}_2$ .

We conclude this section with some remarks concerning the Hall coefficient. In this case the discrepancies between the calculation and the experimental data are especially pronounced.  $\text{CeCu}_2\text{Si}_2$  shows a skew-scattering behavior typical of all heavy-fermion systems and this is not reproduced by the calculation. On the other hand, the Hall coefficient can vary appreciably in magnitude and sign within a set of samples of the same heavy-fermion system. The intricate influence of inter-site spin interactions might be responsible for the strong deviations of the calculations from the experimental data. Nevertheless, the calculations predict in the Fermi-liquid regime a negative quadratic temperature dependence. With increasing temperature the skew-scattering part of the Hall coefficient increases and eventually overcompensates the negative Fermi-liquid contribution. As a result, a low-temperature minimum in the Hall coefficient develops. This is experimentally observed in several heavy-fermion systems and was discussed in more detail in [23].

#### IV. CONCLUSIONS

The electronic transport properties of heavy-fermion systems were calculated on the basis of a semiphenomenological approach to the lattice non-crossing approximation in the limit of infinite local Coulomb repulsion augmented by crystal-field effects. The calculation is able to reproduce the qualitative features of the temperature-dependent resistivity, the magnetoresistivity and the thermoelectric power, as exemplified by a comparison with experimental data of  $\text{CeCu}_2\text{Si}_2$  and  $\text{La}_{0.9}\text{Ce}_{0.1}\text{Cu}_{2.2}\text{Si}_2$ . The skew-scattering characteristic of the temperature dependent Hall coefficient is not reproduced. Nevertheless, the lack of agreement between the experimental data and the calculation could presumably be traced back to secondary effects which are not included in our model. The disorder-induced suppression of coherent scattering in the resistivity and inter-site spin interactions that might especially influence the thermoelectric power and the Hall coefficient are not taken into account.

Within the scope of this approach an extension to include crystal-field excitations to magnetic singlet states can be easily accomplished by adding the respective resistivity or,



more generally, the self-energy contributions of the singlet states as described by Cornut and Coqblin [24]. This permits the calculation of the transport properties of the uranium-based heavy-fermion systems, which tend to be in a  $5f^2$ -state [30].

A more sophisticated transport theory based on the Kubo formalism might be necessary to account for the generally anisotropic band structure and probably an anisotropic hybridization. This might result in a more quantitative agreement between the experimental data and the calculated transport coefficients. However, in our opinion the consideration of non-local quasiparticle interactions is essential in order to account for the observed behavior of the thermopower and Hall coefficient. This is surely beyond the present approach and should be devoted to calculations based on a fully microscopic description of the electronic transport properties in heavy-fermion systems.

#### ACKNOWLEDGMENTS

This work was supported by the Deutsche Forschungsgemeinschaft through SFB 252. Additionally one of us (FBA) was supported by the Deutsche Forschungsgemeinschaft, in part by the National Science Foundation under Grant No. PHY94-07194, and the US Department of Energy, Office of Basic Energy Science, Division of Materials Research. FBA would like to thank the Institute for Theoretical Physics (ITP) in Santa Barbara, California, USA, for its hospitality where part of the work has been performed.

## REFERENCES

- [1] H. Keiter and J. C. Kimball, *Int. J. Magn.* **1**, 233 (1971); N. Grewe and H. Keiter, *Phys Rev. B* **24**, 4420 (1981); H. Keiter and G. Morandi, *Phys Rep.* **109**, 227 (1984).
- [2] e. g. N. E. Bickers, *Rev. Mod. Phys.* **127**, 845 (1987); A. C. Hewson, *The Kondo Problem to Heavy Fermions*, Cambridge University Press, Cambridge (1993).
- [3] N. Grewe, *Z. Phys. B* **52**, 193 (1983); Y. Kuramoto, *Z. Phys. B* **53**, 37 (1983).
- [4] N. Grewe, *Z. Phys. B* **67**, 323 (1987); N. Grewe, Th. Pruschke, and H. Keiter, *Z. Phys. B* **71**, 75 (1988).
- [5] F. B. Anders , N. Grewe, *Europhys. Lett.* **26**, 551 (1994); F. B. Anders, *J. Phys. : Condens. Matter* **7**, 2801 (1995); F. B. Anders, PhD thesis, TH–Darmstadt, Germany (1995), unpublished.
- [6] Th. Pruschke et. al., *Adv. in Phys.* **42**, 187 (1995); A. Georges et. al., *Rep. Mod. Phys.* **68**, 1 (1996);
- [7] D. L. Cox and N. Grewe, *Z. Phys. B* **71**, 321 (1988).
- [8] A. Lorek, F. Anders, and N. Grewe, *Solid State Commun.* **78**, 167 (1991).
- [9] F. B. Anders and D. L. Cox, to be published in *Physica B* (1997) and cond–mat/9609165.
- [10] N. Grewe and B. Welslau, *Solid. State Commun.* **66**, 1053 (1988).
- [11] B. Welslau and N. Grewe, *Ann. Physik* **1**, 214 (1992).
- [12] K. Yamada and K. Yosida in *Theory of Heavy Fermions and Valence Fluctuations*, T. Kasuya and T. Saso (eds. ), p 184, Berlin, Heidelberg, New York, Springer (1985); K. Yamada and K. Yosida, *Prog. Theor. Phys.* **76**, 621 (1986).
- [13] N. Grewe, *Z. Phys. B* **53**, 271 (1983).
- [14] Y. Nagaoka, *Phys. Rev. A* **138**, 1112 (1965); H. Suhl, *Phys. Rev. A* **138**, 515 (1965).

- [15] e. g. G. Rickayzen , *Green's Functions and Condensed Matter*, Academic Press, San Diego (1980).
- [16] e. g. J. M. Ziman, *Principles of the Theory of Solids*, second edition, Cambridge University Press, London (1972).
- [17] e. g. M. Abramowitz and I. Stegun, *Handbook of Mathematical Functions*, ninth edition, Dover Publication Inc. (1972).
- [18] E. A. Goremychkin and R. Osborn, Phys. Rev. B **47**, 14280 (1993); E. A. Goremychkin, A. Yu. Muzychka, and R. Osborn, Sov. Phys. JETP **83**, 738 (1996).
- [19] e. g. N. Grewe and F. Steglich, *Heavy Fermions* in Handbook of the Physics and Chemistry of Rare Earths, volume 14, K. A. Gschneidner Jr. and L. Eyring (eds. ), Elsevier (1991).
- [20] Y. Onuki, T. Hirai, T. Kumazawa, T. Komatsubara, and Y. Oda, J. Phys. Soc. Jpn. **56**, 1454 (1987).
- [21] C. S. Garde, J. Ray, and G. Chandra, Phys. Rev. B **45**, 7217 (1992).
- [22] F. G. Aliev, N. B. Brandt, V. V. Moshchalkov, M. K. Zalyalyutdinov, and V. Kovachik, Sov. Phys. JETP **65**, 509 (1987 ).
- [23] M. Huth, J. Hessert, M. Jourdan, A. Kaldowski, and H. Adrian, Phys. Rev. B **50**, 1309 (1994).
- [24] B. Cornut and B. Coqblin, Phys. Rev. B **5**, 4541 (1972); Y. Lassailly, A. K. Bhattacharjee, and B. Coqblin, Phys. Rev. B **31**, 7424 (1985).
- [25] E. Miranda, V. Dobrosavljević, and G. Kotliar, Phys. Rev. Lett. **78**, 290 (1997).
- [26] A. Amato, D. Jaccard, J. Sierro, P. Haen, P. Lejay, and J. Flouquet, J. Low Temp. Phys. **77**, 195 (1989).

- [27] T. S. Kim and D. L. Cox, Phys. Rev. Lett. **75**, 1622 (1996).
- [28] F. Steglich, B. Buschinger, P. Gegenwart, M. Lohmann, R. Helfrich, C. Langhammer, P. Hellmann, L. Donnevert, S. Thomas, A. Link, C. Geibel, M. Lang, G. Sparn, and W. Assmus, J. Phys. : Condens. Matter **8**, 9909 (1996).
- [29] P. Link, D. Jaccard, and P. Lejay, Physica B **225**, 207 (1996).
- [30] M. Huth, PhD thesis, Darmstadt, Germany (1995), unpublished.